第 49 卷第 6 期　　硅　酸　盐　学　报　　Vol. 49，No. 6
2021 年 6 月　　JOURNAL OF THE CHINESE CERAMIC SOCIETY　　June，2021
http://www.gxyb.cbpt.cnki.net　　DOI：10.14062/j.issn.0454-5648.20200617

综 合 评 述

Sb_2Te_3 基热电薄膜的研究进展

易　文[1,2]，赵永杰[1]，王伯宇[1]，周志方[2]，李亮亮[2]，李静波[1]

(1. 北京理工大学材料学院，北京 100081；2. 清华大学材料学院，北京 100084)

摘　要：基于热电薄膜的微型热电器件在微区制冷、温差发电等领域具有广阔应用前景。具有高功率因子、*ZT* 值的热电薄膜对微型热电器件的性能至关重要。Sb_2Te_3 基材料是室温下性能优异的 p 型热电材料。然而，目前 Sb_2Te_3 基薄膜的热电性能仍然不能满足实际应用的需求。简述了热电材料研究的相关背景，介绍了 Sb_2Te_3 的晶体结构，概述了 Sb_2Te_3 基薄膜的常用制备技术，从提高功率因子和降低热导率 2 方面综述了提高 Sb_2Te_3 基薄膜热电性能的方法。重点介绍了材料组织、微观结构与热电性能的关系，即缺陷、择优取向、纳米颗粒、超晶格、有机无机杂化等对 Sb_2Te_3 基薄膜热电性能的影响。此外，对 Sb_2Te_3 基热电薄膜的发展方向予以展望。

关键词：热电薄膜；碲化锑；热电性能；功率因子；热导率
中图分类号：TB34　　**文献标志码：**A　　**文章编号：**0454–5648(2021)06–1111–14
网络出版时间：2021–04–06

Research Progress on Antimony Telluride Based Thermoelectric Thin Films

YI Wen[1,2], *ZHAO Yongjie*[1], *WANG Boyu*[1], *ZHOU Zhifang*[2], *Li Liangliang*[2], *Li Jingbo*[1]

(1. School of Materials Science and Engineering, Beijing Institute of Technology, Beijing 100081, China;
2. School of Materials Science and Engineering, Tsinghua University, Beijing 100084, China)

Abstract: Micro thermoelectric devices based on thermoelectric films have promising applications in various fields such as micro-zone refrigeration and power generation. Thermoelectric films with high power factor and large *ZT* values are critical materials in these devices. Sb_2Te_3-based materials are outstanding p-type thermoelectric materials at room temperature. However, the thermoelectric properties of Sb_2Te_3-based thin films cannot meet the requirement of practical applications. The research background of thermoelectric materials is briefly introduced, the crystal structure of Sb_2Te_3 is discussed, the preparation techniques of Sb_2Te_3-based thin films are outlined, and the methods of improving the power factor and reducing the thermal conductivity of Sb_2Te_3-based thin films are summarized. In particular, the effects of microstructure on thermoelectric properties are focused on to elucidate the mechanism of improving thermoelectric properties of the films, which includes defects, preferential orientation, nanoparticles, superlattice, organic-inorganic hybridization, and so on. In addition, the future research directions for Sb_2Te_3-based thermoelectric thin films are discussed.

Keywords: thermoelectric thin film; antimony telluride; thermoelectric property; power factor; thermal conductivity

当前，能源危机、全球变暖、环境污染等问题日益严重，因此，寻找资源丰富、环境友好的新能源材料，并实现能源的高效利用至关重要[1−3]。基于 Seebeck 效应和 Peltier 效应，热电材料能够实现热能和电能之间的相互转换，同时热电器件具有无污染、无运动部件、无噪声、易于维护、使用寿命长、可串并联等优点[4]，在温差发电、固态制冷、无线传感等方面表现出优异的功能特性，在新能源、电

收稿日期：2020–08–17。　修订日期：2020–09–22。
基金项目：国家自然科学基金(51972029)；国家重点研发计划(2016YFA0201003)。
第一作者：易　文(1996 —)，男，硕士研究生。
通信作者：李静波(1969 —)，男，博士，教授。
李亮亮(1980 —)，男，博士，副研究员。

Received date: 2020–08–17.　**Revised date:** 2020–09–22.
First author: YI Wen (1996 –), male, Master candidate.
E-mail: yiwen18@126.com
Correspondent author: LI Jingbo(1969 –), male, Ph.D., Professor;
LI Liangliang(1980–), male, Ph.D., Associate Professor.
E-mail: lijb@bit.edu.cn; liliangliang@mail.tsinghua.edu.cn

子信息、医疗器械、航空航天、国防等多领域具有显著的应用价值[5–6]。热电材料的性能一般用无量纲优值(*ZT*)来衡量。*ZT* 的计算公式为：

$$ZT = S^2\sigma T / \kappa \quad (1)$$

其中：*S* 为 Seebeck 系数；σ 为电导率；*T* 为绝对温度；κ 为热导率；$S^2\sigma$ 为功率因子。热电材料的热导率 κ 由载流子热导率 κ_e 和晶格热导率 κ_L 组成[7–8]，即：

$$\kappa = \kappa_e + \kappa_L \quad (2)$$

由式(1)可知，提高热电材料的 *ZT* 值，需要提高材料的 Seebeck 系数和电导率，同时降低材料的热导率，而这 3 个参数相互耦合，难以实现单一调控[1,9]。理论研究发现，材料尺度降低到纳米级别时所产生的量子限域效应为单独调控电导率、Seebeck 系数和热导率提供了可能[10–14]。

随着微机电系统、物联网技术的发展以及各种智能可穿戴设备的不断涌现，对设备的可持续供电提出了新的要求。传统电池存在需要定期更换、充电和维修的缺点。基于热电薄膜的微型热电器件能够收集周围环境热量实现长时间供电，同时还具有柔性好、体积小、适应于多种复杂环境等优点，在物联网传感器、移动电子等领域具有广阔应用前景[15–18]。

Sb_2Te_3 属于窄带隙半导体(E_g<0.3 eV)[19]。Sb_2Te_3 基热电材料一般为 p 型，室温下具有优异的热电性能[20–23]。近年来，Sb_2Te_3 基薄膜受到科研工作者的广泛关注。热蒸发、溅射、电化学沉积、分子束外延(MBE)、脉冲激光沉积(PLD)、化学气相沉积(CVD)等多种技术均可用于制备 Sb_2Te_3 基薄膜。通过组织调控，如第二相纳米颗粒、择优取向、超晶格结构等，可以显著改善 Sb_2Te_3 基薄膜的热电性能。Kim 等[24]采用脉冲激光沉积方法在 $Bi_{0.5}Sb_{1.5}Te_3$ 薄膜中引入 Te 纳米颗粒，利用能量过滤效应提高薄膜性能。当 Te 纳米颗粒从 0%(体积分数)增加到~15%时，薄膜 Seebeck 系数从 170.00 μV/K 提高到 250.00 μV/K，功率因子从 1.55 mW/(m·K^2)提高到 2.22 mW/(m·K^2)。Tan 等[25]采用一种新颖的电场辅助磁控溅射方法制备了高度(0 1 5)取向的 Sb_2Te_3 薄膜。在 30 V 外电场作用下，该薄膜的室温 *ZT* 值达到了 1.75。Venkatasubramanian 等[26]通过金属有机化学气相沉积制备了 p 型 Bi_2Te_3/Sb_2Te_3 超晶格薄膜。该薄膜晶格热导率最小值为~0.22 W/(m·K)，而对应的 Sb_2Te_3 和 Bi_2Te_3 的晶格热导率分别为~0.96 W/(m·K)和~1.05 W/(m·K)。

为了满足实际应用需求，Sb_2Te_3 基薄膜的热电性能仍需进一步提升，首先简述了 Sb_2Te_3 材料的晶体结构，然后介绍了 Sb_2Te_3 基薄膜的常用制备技术，之后从提高功率因子和降低热导率 2 个角度总结了提高 Sb_2Te_3 基薄膜热电性能的方法，最后对 Sb_2Te_3 薄膜未来的研究方向予以展望。

1 Sb_2Te_3 的晶体结构

图 1 为 Sb_2Te_3 的晶体结构示意图。Sb_2Te_3 属于三方晶体结构，空间群为 $R\bar{3}m$ [27–28]，沿六方坐标系下 *c* 轴方向呈周期性层状结构。该周期性层状结构单元由五层原子层组成，原子层的顺序为 Te(Ⅰ)-Sb-Te(Ⅱ)-Sb-Te(Ⅰ)，其中 Te(Ⅰ)与 Sb 之间以共价键和离子键相连，Te(Ⅱ)与 Sb 之间以共价键相连，相邻的 Te(Ⅰ)与 Te(Ⅰ)通过 van der Waals 键相连[27–30]。

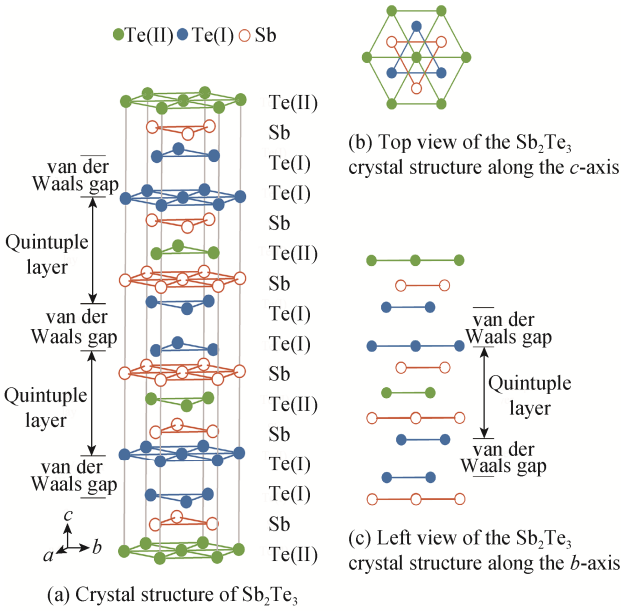


图 1 Sb_2Te_3 晶体结构示意图

Fig. 1 Crystal structure of Sb_2Te_3

Sb_2Te_3 的结构特点使 Sb 原子和 Te(Ⅱ)原子受到较大的束缚，而 Te(Ⅰ)原子受到的束缚相对较弱，材料容易出现 Te 空位。由于 Sb 与 Te 的原子半径 γ 和电负性 χ 都比较接近(γ_{Sb}=140 pm，γ_{Te}=136 pm；χ_{Sb}=2.05，χ_{Te}=2.10)，多余的 Sb 原子容易取代 Te 原子形成反位缺陷 Sb'_{Te}，导致 Sb_2Te_3 表现出较强的 p 型传导[27]，如式(3)所示：

$$2Sb + 3Te = 2Sb'_{Te} + 6h + V^{\bullet\bullet}_{Te} + 2V'''_{Sb} + 3/2Te_2(g) \quad (3)$$

其中：h 为空穴；$V^{\bullet\bullet}_{Te}$ 为 Te 空位；V'''_{Sb} 为 Sb 空位；$Te_2(g)$为挥发的 Te[31–33]。

研究发现，Sb_2Te_3 的层状结构导致该材料的电导率和热导率存在很大的各向异性，两者在垂直于 *c* 轴方向的数值均高于平行于 *c* 轴方向的数值，而 Seebeck

系数几乎没有各向异性[34–38]。因此，调控晶体取向为解耦各个热电参数提供了一个可能的途径。

2　Sb_2Te_3 基薄膜的制备技术

Sb_2Te_3 基薄膜可以通过热蒸发、溅射、电化学沉积、MBE、PLD、CVD 等多种技术制备。热蒸发、溅射和电化学沉积是常用技术，它们所使用的设备相对简单且易于操作[39]。表 1 总结了不同技术制备的 Sb_2Te_3 基薄膜的热电性能。热蒸发的沉积速率高，膜厚可控，但是薄膜与基板附着力较小[14]。与热蒸发相比，溅射沉积的 Sb_2Te_3 薄膜致密度更高，薄膜与基板的附着力更好，薄膜功率因子略高，但缺点是其沉积速率比热蒸发低，而且靶材利用率低。电化学沉积不需要真空条件，成本低，沉积速度快[40–43]，但是薄膜的沉积受电流、电压、温度、溶剂、溶液的 pH 值、浓度、电极表面状态等多种因素的影响，因此薄膜的成分控制和结构调控较为困难[14]。由表 1 可知，与热蒸发和溅射相比，电化学沉积制备的 Sb_2Te_3 基薄膜的功率因子一般更低。

MBE 可在高真空或者超高真空的条件下制备高质量薄膜，能够严格控制薄膜厚度、成分、结构和掺杂浓度，但是 MBE 存在设备昂贵、维修费用高、沉积速率低等问题[14]。PLD 一个突出的优点是能够保持薄膜和靶材成分的一致性[44–47]，避免因 Te 的高温易挥发性而导致的薄膜成分偏离化学计量比，但是采用 PLD 制备的薄膜均匀性欠佳，因此难以制备大面积薄膜[14]。CVD 沉积的薄膜一般纯度高、残余应力小、结晶性好、沉积速率高，但是部分反应气体易燃或有一定毒性。

表 1　不同方法制备的 Sb_2Te_3 基薄膜的热电性能

Table 1　Thermoelectric properties of Sb_2Te_3 based thin films deposited by different preparation techniques

Film	Preparation technique	Substrate	Film thickness/ nm	σ/ ($S\cdot cm^{-1}$)	S/ ($\mu V\cdot K^{-1}$)	$S^2\sigma$/ ($mW\cdot m^{-1}\cdot K^{-2}$)	κ/ ($W\cdot m^{-1}\cdot K^{-1}$)	ZT	Reference
Sb_2Te_3	Evaporation	SiO_2/Si(100)	1 000	628.14	230.07	3.32			[48]
Sb_2Te_3	Evaporation	SiO_2 glass	2 500	790.00	187.00	2.76	0.94	0.88	[49]
$Bi_{0.4}Sb_{1.6}Te_3$	Evaporation	Glass	190	640.00	236.00	3.56			[50]
$Bi_{1.5}Sb_{0.5}Te_3$	Evaporation	SiO_2 glass	5 000	760.00	226.00	3.88	0.91	1.28	[51]
Sb_2Te_3	Magnetron sputtering	Conductive glass	1 500	779.42	261.56	5.33	0.91	1.75	[25]
$Bi_{0.5}Sb_{1.5}Te_3$	Magnetron sputtering	Glass	563	800.00	219.00	3.80			[52]
$Bi_{0.5}Sb_{1.5}Te_3$	Magnetron sputtering	AlN	1 300	1 230.00	198.00	4.82			[53]
Sb_2Te_3	Magnetron sputtering	SiO_2 glass	1 000	820.00	229.00	4.30	1.06	1.22	[54]
$Bi_{0.5}Sb_{1.5}Te_3$	Magnetron sputtering	AlN	490	1 460.00	191.30	5.34			[55]
Sb_2Te_3	Ion beam sputtering	BK7 glass	330	2 361.00	161.00	6.12			[56]
Sb_2Te_3	Electrochemical deposition	Ti/Cu/Ti/Si	10 000	281.69	441.20	5.48			[57]
Sb_2Te_3	Electrochemical deposition	Cr/Au/Si	50 000	400.00	170.00	1.12			[58]
Sb_2Te_3	Electrochemical deposition	Stainless steel (SUS304)	300	1 032.00	115.00	1.36			[41]
$(Bi_xSb_{1-x})_2Te_3$	Electrochemical deposition	Au/Pt/Cr/Si or stainless steel	20 000	400.00	182.00	1.32	1.00	0.40	[59]
Sb_2Te_3	MBE	GaSb/Si(111)	200	3 238.30	138.00	6.17			[60]
Sb_2Te_3	MBE	BaF_2(111) and SiO_2/Si	1 000	1 696.00	130.00	2.90			[61]
$Bi_{0.5}Sb_{1.5}Te_3$	PLD	Fused silica	180	736.98	194.00	2.78			[62]
$Bi_{0.4}Sb_{1.6}Te_3$	PLD	SiO_2/Si	1 250	2 759.36	94.90	2.49	1.00	0.75	[63]
$Bi_{0.5}Sb_{1.5}Te_3$	PLD	MgO	575	361.00	250.00	2.22	1.09	0.61	[24]
Sb_2Te_3	Plasma-enhanced CVD	Graphene/SiO_2/ Si(001)	>200	1 854.41	139.17	3.59			[64]

MBE is molecular beam epitaxy; PLD is pulsed laser deposition; CVD is chemical vapor deposition.

3 提高功率因子

Sb_2Te_3 薄膜可以通过多种技术制备，但是其热电性能还难以满足实际应用的需求，需要进一步提高 *ZT* 值。提高热电薄膜的功率因子是获得高 *ZT* 值的一种常用方法。由式(1)可知，提高电导率和 Seebeck 系数能够改善功率因子。

3.1 提高电导率

电导率 σ 可以表示为:

$$\sigma = 1/\rho = ne\mu \tag{4}$$

其中：ρ 为电阻率；n 为载流子浓度；e 为电子电荷(1.602×10^{-19} C)；μ 为载流子迁移率[65]。由式(4)可知，提高热电材料的电导率，需要提高载流子迁移率或载流子浓度。

调节退火温度或者沉积温度是提高薄膜载流子迁移率的有效方法。载流子迁移率与材料中的多种散射机构密切相关[66–67]，在 Sb_2Te_3 薄膜中主要散射机构是电离杂质散射和晶界散射。室温沉积的 Sb_2Te_3 薄膜往往电离杂质多，结晶度低，晶界多，因此性能不佳。对薄膜进行退火热处理或调节薄膜沉积温度可以有效地降低电离杂质，提高薄膜结晶度，增加晶粒尺寸，减少晶界，从而减少电离杂质散射和晶界散射，提高载流子迁移率、电导率和功率因子[42,62,68–75]。Fang[70]等、Fan[68]等、Kim[76]等研究了退火温度对 Sb_2Te_3 基薄膜载流子迁移率的影响。实验发现室温沉积所制备薄膜的载流子迁移率在退火后明显提高，而且随着退火温度的升高不断增加。综合文献报道结果，为获得最高的功率因子，Sb_2Te_3 薄膜的最佳退火温度一般为 523~673 K，如表 2 所示。此外，Sb_2Te_3 薄膜的最佳沉积温度一般为 493~543 K，如表 3 所示。

表 2 Sb_2Te_3 薄膜的最佳退火温度及室温热电性能

Table 2 Optimal annealing temperatures of Sb_2Te_3 thin films and corresponding thermoelectric properties at room temperature

Film	Preparation technique	Optimal annealing temperature/K	σ/(S·cm^{-1})	S/(μV·K^{-1})	$S^2\sigma$/(mW·m^{-1}·K^{-2})	Reference
Sb_2Te_3	Magnetron sputtering	573	650.00	125.00	1.02	[39]
Sb_2Te_3	Electrodeposition	573	1 304.00	100.00	1.36	[41]
Sb_2Te_3	Magnetron sputtering	523	1 170.00	123.90	1.80	[70]
Sb_2Te_3	Ion beam sputtering	673	2 010.00	106.00	2.26	[68]
$Bi_{0.5}Sb_{1.5}Te_3$	Magnetron sputtering	673	380.00	178.00	1.20	[76]

表 3 Sb_2Te_3 薄膜的最佳沉积温度及室温热电性能

Table 3 Optimal deposition temperatures of Sb_2Te_3 thin films and corresponding thermoelectric properties at room temperature

Film	Preparation technique	Optimal deposition temperature/K	σ/(S·cm^{-1})	S/(μV·K^{-1})	$S^2\sigma$/(mW·m^{-1}·K^{-2})	Reference
Sb_2Te_3	Magnetron sputtering	523	2 660.00	113.00	3.26	[77]
Sb_2Te_3	Evaporation	493	1 000.00	133.00	1.78	[78]
Sb_2Te_3	Evaporation	503	960.00	171.00	2.80	[79]
Sb_2Te_3	Evaporation	543	800.00	149.00	1.78	[80]

由于 Te 的蒸气压较高，如果退火温度或沉积温度过高，Te 元素则容易蒸发，从而改变薄膜成分，增加薄膜缺陷，降低材料的热电性能[39,81–82]。为了获得符合化学计量比的 Sb_2Te_3 基薄膜，可以在磁控溅射沉积时采用 Te 靶与其他靶材共溅的方式[54,83–84]，或者在蒸发沉积中采用 Te 源与其他蒸发源共蒸发的方式[51,78]来增加 Te 的沉积量，从而弥补 Te 的损失。此外，改变退火时的气氛也是一种减少 Te 蒸发的方法。Schumacher 等[59]发现在 Te 气氛下退火，$(Bi_xSb_{1-x})_2Te_3$ 薄膜中 Te 的蒸发量明显减少。

薄膜的择优取向也会影响载流子迁移率。如前所述，Sb_2Te_3 基材料的电导率具有明显的各向异性，载流子沿不同晶面的传输性能差异较大，因此可以通过控制薄膜生长的取向来优化载流子迁移率。表 4 和图 2a～图 2d 列举了文献报道的无序薄膜、(0 1 5)和(0 0 *l*)取向薄膜的热电性能。从无序薄膜到(0 1 5)取向再到(0 0 *l*)取向的薄膜，载流子迁移率大幅度增加，电导率显著提高，与此同时，Seebeck 系数也有明显改善。因此，薄膜的功率因子有大幅度提升。图 2e 是 Sb_2Te_3 (0 0 *l*)和(0 1 5)晶面的示意图[85]。理论计算表明，沿(0 0 *l*)方向的原子密度比沿(0 1 5)方向的密度小，载流子沿(0 0 *l*)方向受到原子散射更

少，因此沿该方向择优生长的薄膜具有更高的载流子迁移率[52]。

在薄膜的制备过程中，沉积温度[52,54]、沉积速率[49,86]、气体压强[87−88]、退火温度[53]等因素均会影响薄膜的择优取向，调控这些参数能够获得高度取向的 Sb_2Te_3 薄膜。Mu 等[52]用磁控溅射方法在 473~723 K 范围内制备了不同沉积温度的 $Bi_{0.5}Sb_{1.5}Te_3$ 薄膜，发现随着沉积温度的增加，薄膜择优取向经历了从(0 1 5)到(1 0 10)再到(0 0 *l*)的转变，载流子迁移率从 4.00 $cm^2/(V·s)$ 增加到 62.50 $cm^2/(V·s)$，功率因子从 0.10 $mW/(m·K^2)$增加到 3.80 $mW/(m·K^2)$。Zhu 等[53]用磁控溅射方法在 723 K 制备了(0 1 5)取向的 $Bi_{0.5}Sb_{1.5}Te_3$ 薄膜。在 573 K 退火后，薄膜从(0 1 5)取向转变成(0 0 *l*)取向，载流子迁移率从 36.10 $cm^2/(V·s)$增加到 106.30 $cm^2/(V·s)$，功率因子从 1.42 $mW/(m·K^2)$增加到 4.82 $mW/(m·K^2)$。

除了提高载流子迁移率，提高材料的载流子浓度也能获得较高的电导率。适当的元素掺杂能够有效调控热电材料的能带结构，这是一个提高载流子浓度的常用方法[89−92]。表 5 列举了 Cu 掺杂前后 Sb_2Te_3 基块体和薄膜的热电性能。Cu 掺杂有效提高了 Sb_2Te_3 材料的载流子浓度，使得材料的电导率、功率因子和 *ZT* 值显著提升[93−96]。目前，有关掺杂对 Sb_2Te_3 薄膜热电性能影响的研究尚不充分，在该领域进一步探索有望获得性能优异的 Sb_2Te_3 基薄膜。

表 4　具有不同择优取向 Sb_2Te_3 薄膜的室温热电性能

Table 4　Thermoelectric properties of Sb_2Te_3 thin films with different preferential orientations at room temperature

Reference	Preferential orientation	$n\times10^{19}/cm^{-3}$	$\mu/(cm^2·V^{-1}·s^{-1})$	$\sigma/(S·cm^{-1})$	$S/(\mu V·K^{-1})$	$S^2\sigma/(mW·m^{-1}·K^{-2})$
[54]	Ordinary	12.60	13.00	250.00	113.00	0.32
	(0 1 5)	9.50	27.00	410.00	157.00	1.01
	(0 0 *l*)	3.10	161.00	820.00	229.00	4.30
[97]	Ordinary	9.10	20.00	280.00	175.00	0.86
	(0 1 5)					
	(0 0 *l*)	4.20	89.00	670.00	214.00	3.07
[52]	Ordinary	5.20	4.00	30.00	189.00	0.10
	(0 1 5)	7.00	16.40	180.00	189.00	0.60
	(0 0 *l*)	7.90	62.50	800.00	219.00	3.80

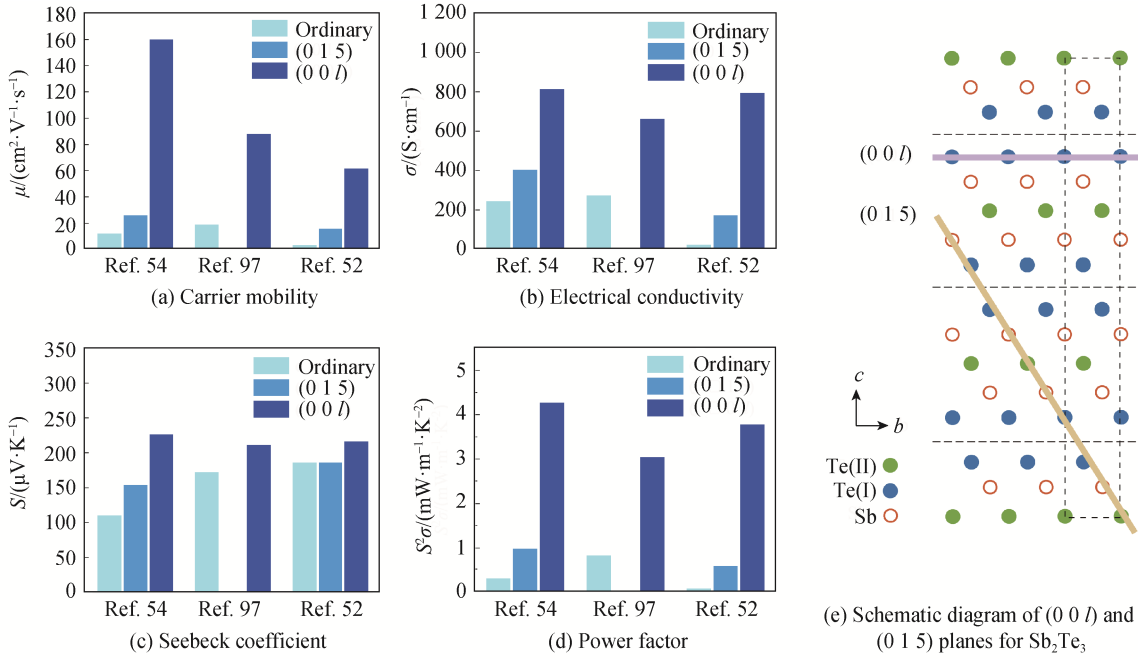


图 2　具有不同择优取向 Sb_2Te_3 薄膜的室温热电性能[52,54,97]及 Sb_2Te_3 (0 0 *l*)和(0 1 5)晶面示意图

Fig. 2　thermoelectric properties of Sb_2Te_3 thin films with different preferential orientations at room temperature[52,54,97] and the schematic diagram of (0 0 *l*) and (0 1 5) planes for Sb_2Te_3

表 5 Cu 掺杂对 Sb_2Te_3 基材料热电性能的影响

Table 5 Effects of Cu doping on the thermoelectric properties of Sb_2Te_3 based materials

Reference	Material	$n\times10^{19}$/cm^{-3}	σ/(S·cm^{-1})	$S^2\sigma$/(mW·m^{-1}·K^{-2})	ZT	Type
[94]	$Bi_{0.5}Sb_{1.5}Te_3$	2.00	400.00	2.03	0.70	Bulk
	$Cu_{0.005}Bi_{0.5}Sb_{1.495}Te_3$	4.00	1 400.00	3.36	0.95	
[95]	$Bi_{0.5}Sb_{1.5}Te_3$	2.50	90.00	0.25	0.15	Bulk
	$Cu_{0.6}(Bi_{0.5}Sb_{1.5}Te_3)_{99.4}$	6.50	1 100.00	2.50	1.20	
[96]	Sb_2Te_3	12.69	320.00	0.27 (480 K)		Thin film
	$Cu_{4.4}(Sb_2Te_3)_{95.6}$	19.46	460.00	0.38 (480 K)		

3.2 提升 Seebeck 系数

简并半导体的 Seebeck 系数根据 Mott 关系可表示为：

$$S=\frac{\pi^2k_B^2}{3e}T\{\frac{\mathrm{d}[\ln(\sigma(E))]}{\mathrm{d}E}\}_{E=E_F} \tag{5}$$

$$=\frac{\pi^2k_B^2}{3e}T\{\frac{\mathrm{d}[\ln(n(E))]}{\mathrm{d}E}+\frac{\mathrm{d}[\ln(\mu(E))]}{\mathrm{d}E}\}_{E=E_F} \tag{6}$$

其中：k_B 为 Boltsman 常数(1.380×10^{-23} J/K)；E 为电子能量；E_F 为 Fermi 能。简并半导体中的载流子迁移率可表示为：

$$\mu(E)\approx\frac{e\tau(E)}{m^*} \tag{7}$$

其中 $\tau(E)$为载流子弛豫时间；m*为载流子有效质量[98–99]。根据式(6)和式(7)可知，提高 d[ln($\tau(E)$)]/dE 将会提高 d[ln($\mu(E)$)]/dE，从而提高 Seebeck 系数。

理论和实验发现，能量过滤效应可以提高 d[ln($\tau(E)$)]/dE[98]。在材料中引入第二相纳米颗粒会引起能带弯曲，从而在纳米颗粒和基体之间的界面处形成势垒，使能量较低的载流子被选择性散射，该效应即能量过滤效应[5,100–101]，如图 3a 所示。图 3b～图 3d 分别展示了 Sb、Ag、Pt、Te 纳米颗粒的引入所产生的能量过滤效应对薄膜载流子迁移率、Seebeck 系数和功率因子的影响。在这些纳米颗粒与 Sb_2Te_3 的界面处产生了能量过滤效应，因而降低了薄膜的载流子迁移率，提高了薄膜的 Seebeck 系数和功率因子[99,102–104]。此外，在材料中引入 Ag_2Te 等[105–107]纳米颗粒也产生了类似的效果。这是由于大量能量较低的载流子在纳米颗粒与 Sb_2Te_3 之间的界面处被散射，抑制了载流子的传输，使得载流子迁移率下降。这个过程会使载流子弛豫时间对能量的依赖性增强，即在 Fermi 能级上的 d[ln($\tau(E)$)]/dE 增加，从而导致 Seebeck 系数和功率因子的提高[99,102,107–108]。

此外，实验发现某些室温沉积的非晶 Sb_2Te_3 薄膜在 373 K 及以下进行退火处理后，其 Seebeck 系数能达到 300.00~600.00 μV/K。如果增加退火温度，Seebeck 系数急剧下降至 200.00 μV/K 以下[109–112]。例如，Kim 等[110]用电化学沉积方法在室温制备了 Sb_2Te_3 非晶薄膜，其 Seebeck 系数约为 170.00 μV/K。在 343 K、5%H_2+95%N_2 气氛下退火 30 min 后 Seebeck 系数提高至 480.00 μV/K。然而，当退火温度增加到 473 K 时，Seebeck 系数下降至 38.00 μV/K。经实验分析，发现在 343 K 退火时，基体中形成了 γ-SbTe 相，在该相与 Sb_2Te_3 的界面处产生的能量过滤效应提高了 Seebeck 系数。在 473 K 退火时，薄膜完全晶化，γ-SbTe 相消失，因此 Seebeck 系数下降。如果通过其他方法能稳定这种两相共存的微观组织结构，同时提高电导率，将有望获得性能优越且结构稳定的 Sb_2Te_3 薄膜。

4 降低热导率

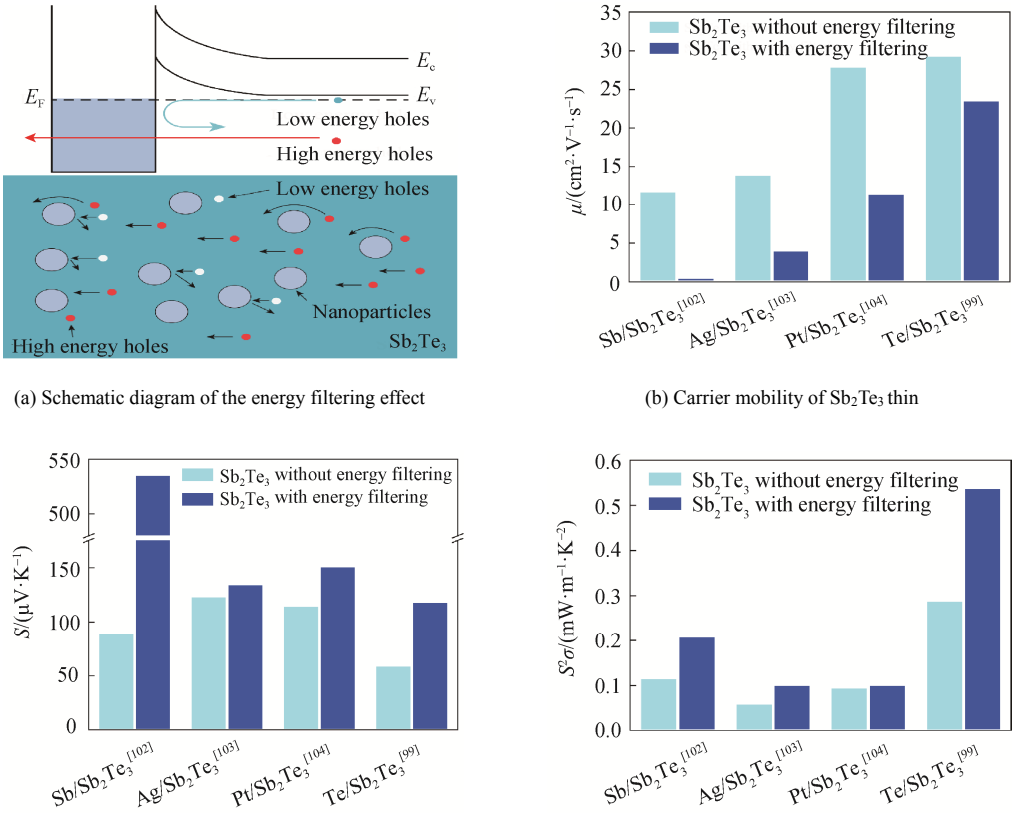
提高薄膜 ZT 值的另外一个途径是降低热导率。图 4 总结了 3 种降低 Sb_2Te_3 薄膜热导率的方法，分别为 Bi_2Te_3/Sb_2Te_3 超晶格构造、有机无机杂化和 Bi_2Te_3 - Sb_2Te_3 固溶。

超晶格结构是一种公认的能显著降低薄膜热导率的方法[113–114]。超晶格材料是由两种或多种晶格匹配良好的材料周期交替沉积构成。金属有机化学气相沉积[115–116]、MBE[117–118]、PLD[44]、电化学沉积[119]、磁控溅射[120]等方法都可以用于制备超晶格材料。图 5 为 Bi_2Te_3/Sb_2Te_3 超晶格结构的示意图[121–122]。

超晶格结构具有各向异性，其热导率降低的机制在面内和面外方向存在差异。在面内方向，主要机制是界面漫散射效应[123–125]，而在面外方向，主要机制是声子相干导热和界面漫散射效应[126–128]。对于 Bi_2Te_3/Sb_2Te_3 超晶格，其面外方向热导率的降低比面内方向更显著[113]。图 6 将 Bi_2Te_3/Sb_2Te_3 超晶格与类似体系块体或薄膜的面外热导率进行了对比。由图 6 可见，Bi_2Te_3/Sb_2Te_3 超晶格面外方向热导率为 0.11~0.31 W/(m·K)，远低于块体和薄膜的面

外热导率[44,115,129]。

超晶格周期对晶格热导率也有较大影响。图 7 中空心点曲线显示了 Bi_2Te_3/Sb_2Te_3 超晶格晶格热导率随周期的变化关系[26]。当超晶格周期为 2 nm 左右时，Bi_2Te_3/Sb_2Te_3 超晶格的晶格热导率接近固溶体 $BiSbTe_3$ 的晶格热导率。随着超晶格周期增加，晶格热导率降低。当周期为 5 nm 时，Bi_2Te_3/Sb_2Te_3 超晶格的晶格热导率最低，为 0.22 W/(m·K)。之后，晶格热导率将随着周期增加而增加，甚至会超过固溶体 $BiSbTe_3$ 的晶格热导率。

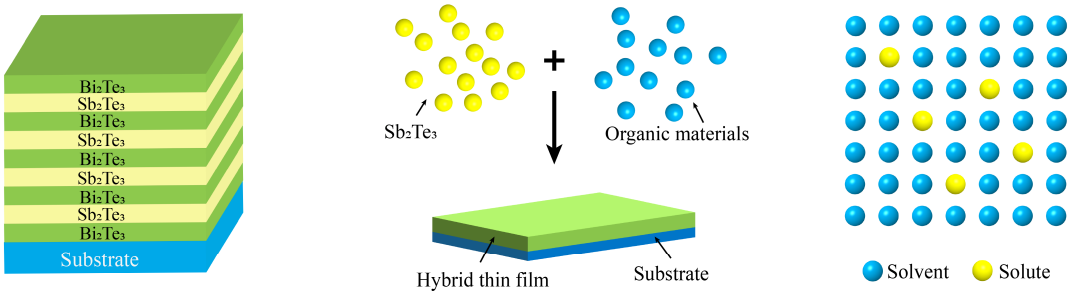


(a) Schematic diagram of the energy filtering effect　(b) Carrier mobility of Sb_2Te_3 thin

(c) Seebeck coefficient　(d) Power factor

图 3　能量过滤效应和室温下有无能量过滤效应的 Sb_2Te_3 薄膜的载流子迁移率、Seebeck 系数和功率因子[99,102–104]

Fig. 3　Schematic diagram of the energy filtering effect and carrier mobility, Seebeck coefficient and power factor of Sb_2Te_3 thin films with and without the energy filtering effect, respectively [99,102–104]



(a) Synthesis of Bi_2Te_3/Sb_2Te_3 superlattice　(b) Organic–inorganic hybridization　(c) Synthesis of Bi_2Te_3–Sb_2Te_3 solid solution

图 4　3 种降低 Sb_2Te_3 薄膜热导率的方法

Fig. 4　Three methods to reduce the thermal conductivity of Sb_2Te_3 thin films

超晶格不仅能有效降低热导率，而且可以改善电学性能。由于在面外方向受到能量过滤效应[130]、热离子发射[131]等因素的影响，面内方向 Fermi 能级附近的态密度显著增加[132]，使得超晶格面外和面内的电学性能都有所提高。Venkatasubramaniam 等[115]发现，与 $(Bi_{0.5}Sb_{0.5})_2Te_3$ 合金相比，Bi_2Te_3/Sb_2Te_3 超晶格面内方向的载流子散射更小，因此面内空穴迁移率高达 ~420.00 $cm^2/(V·s)$，远高于 $(Bi_{0.5}Sb_{0.5})_2Te_3$ 合金的空穴迁移率(~88.00 $cm^2/(V·s)$)。另一方面，实验数据显示两者电导率相同，由于超晶格的迁移率更高，则其载流子浓度更低，因此，其 Seebeck 系数更高。Bi_2Te_3/Sb_2Te_3 超晶格的 Seebeck 系数最大为 260 μV/K,而 $(Bi_{0.5}Sb_{0.5})_2Te_3$ 的 Seebeck 系数仅为~97.00 μV/K。由于 Bi_2Te_3/Sb_2Te_3 超晶格降低了热导率并提高了功率因子，因此制备超晶格薄膜将获得优异的热电性能。

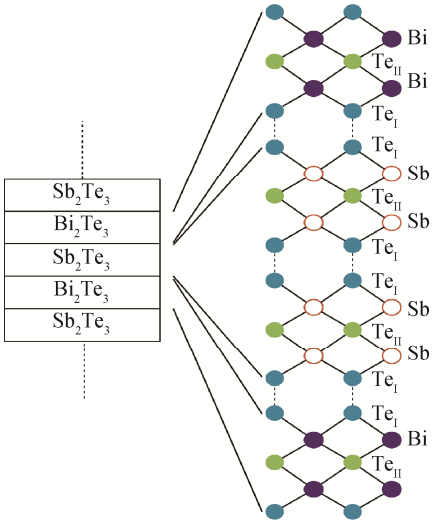


图 5 Bi_2Te_3/Sb_2Te_3 超晶格晶体结构示意图

Fig. 5 Schematic diagram of the crystal structure of the Bi_2Te_3/Sb_2Te_3 superlattice

有机无机杂化是另一种降低热导率的有效方法。利用复合技术，将电学性能良好的 Sb_2Te_3 与低热导率的有机化合物复合，能够实现优势互补。在不显著影响电学性能的情况下，降低 Sb_2Te_3 的热导率，从而获得较高的 *ZT* 值[133]。实验发现，将 Sb_2Te_3 与 CH_3NH_3I 复合能有效降低 Sb_2Te_3 薄膜的热导率[134–135]。例如，Wei 等[135]用热蒸发方法制备了 Sb_2Te_3/CH_3NH_3I 杂化薄膜，经过退火处理后，杂化薄膜热导率为 0.68 W/(m·K)，而纯的 Sb_2Te_3 薄膜热导率为 1.25 W/(m·K)。这是因为 Sb_2Te_3/CH_3NH_3I 的界面有效散射了声子，再加上薄膜中空位和晶界对声子的散射，使得杂化薄膜的热导率降低。此外，在 CH_3NH_3I 与 Sb_2Te_3 的界面处产生了能量过滤效应，使得 Seebeck 系数也得到了提高。杂化薄膜室温 Seebeck 系数为 156.12 μV/K，而纯的薄膜 Seebeck 系数仅为 34.31 μV/K。

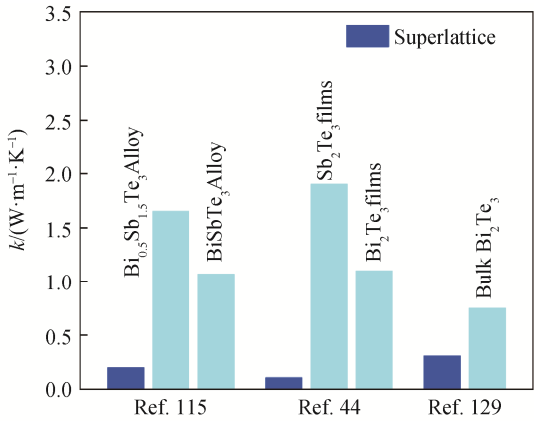


图 6 Bi_2Te_3/Sb_2Te_3 超晶格与类似体系块体或薄膜的面外方向热导率的比较[44,115,129]

Fig. 6 Comparison of the cross-plane lattice thermal conductivity of the Bi_2Te_3/Sb_2Te_3 superlattice and other materials[44,115,129]

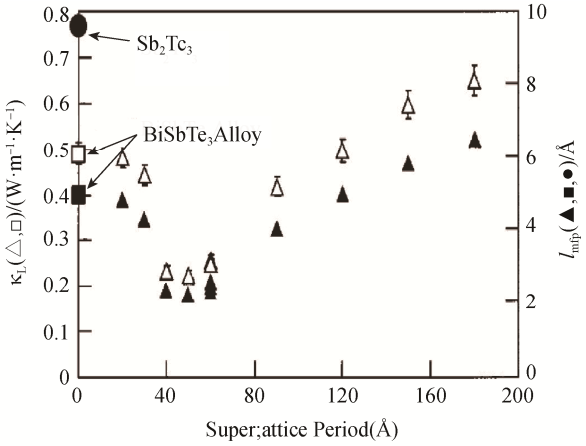


图 7 晶格热导率随 Bi_2Te_3/Sb_2Te_3 超晶格周期的变化(空心点)[26]

Fig. 7 Dependence of the lattice thermal conductivity on the period of Bi_2Te_3/Sb_2Te_3 superlattices (empty dots)[26]

此外，制备 Bi_2Te_3–Sb_2Te_3 固溶体薄膜也可以降低 Sb_2Te_3 薄膜的热导率。Bi_2Te_3 与 Sb_2Te_3 有类似的晶体结构。将 Bi_2Te_3 固溶到 Sb_2Te_3 体系中，会在 Sb_2Te_3 中引入大量点缺陷，从而引起晶格畸变，对声子的散射作用增强，因而显著降低晶格热导率。此外，由于空穴受到的散射作用较小，电学性能不会明显降低[89,136]。Rieger 等[137]用物理气相沉积(PVD)制备了沿 *c* 轴外延生长的 $(Sb_{1-x}Bi_x)_2Te_3$

(x=0.00, 0.07, 0.12, 0.24, 1.00)薄膜。当 x 为 0.00 和 1.00 时，室温下的面外热导率分别为~2.20 W/(m·K)和~1.50 W/(m·K)。随着 x 从 0.00 增加到 0.24，面外热导率不断下降。当 x 为 0.24 时，面外热导率达到最低值，即~0.60 W/(m·K)。

目前准确测量薄膜热导率仍是一个挑战，薄膜热导率测试过程中不必要的热损失和接触热阻都会给测试结果带来一定的误差[138−139]。尽管如此，从上述文献报道的结果看，Bi_2Te_3/Sb_2Te_3 超晶格、有机无机杂化薄膜、Bi_2Te_3 - Sb_2Te_3 固溶体薄膜的热导率仍然低于纯 Sb_2Te_3 薄膜的热导率。因此，上述 3 种方法能够降低 Sb_2Te_3 基薄膜的热导率。

5　总结与展望

Sb_2Te_3 基薄膜是一种温室热电性能优异的材料，其制备方法包括热蒸发、溅射、电化学沉积、MBE、PLD、CVD 等。从提高电导率、提升 Seebeck 系数和降低热导率 3 个方面介绍了优化 Sb_2Te_3 基薄膜热电性能的方法。提高电导率的方法包括热处理、取向控制和掺杂。热处理和取向控制可以减少载流子散射，从而提高载流子迁移率，而在薄膜中掺杂合适的元素能够提高载流子浓度。提升 Seebeck 系数主要是通过能量过滤效应实现。在 Sb_2Te_3 基体中引入纳米颗粒可以产生能量过滤效应，使得载流子弛豫时间对能量的依赖性增加，从而提升 Seebeck 系数。Bi_2Te_3/Sb_2Te_3 超晶格、有机无机杂化和 Bi_2Te_3−Sb_2Te_3 固溶是降低热导率的有效方法。超晶格由于其特殊的结构能够有效散射声子，使热导率显著降低。通过有机无机杂化，将电学性能良好的 Sb_2Te_3 与低热导率的有机化合物复合，能实现不同材料的优势互补。将 Bi_2Te_3 与 Sb_2Te_3 固溶，会在 Sb_2Te_3 中引入大量的点缺陷，从而强烈散射声子。

上述方法一般着眼于优化 Sb_2Te_3 薄膜的某个性能参数。但热电材料的电学和热学性能参数相互耦合，因此难以同时优化多个性能参数。例如：提高载流子浓度，往往能够提高电导率，但是会降低 Seebeck 系数[1,5]。提高电导率，能够提高功率因子，但是会导致载流子热导率增大，从而增加总热导率[140]。缺陷能降低晶格热导率，但是也可能会降低载流子迁移率[21,141−142]。因此，未来需要进一步探索协同优化多个热电性能参数的方法。超晶格薄膜虽然成本高，工艺复杂，但是它利用高界面密度增加了声子散射，降低了热导率，同时利用量子限域效应、能量过滤效应、热离子发射等提高了电学性能，使多个热电参数均得到了优化[108,113,115−116]。此外，制备纳米复合材料的方法能够通过优化能带结构和微观结构来提高基体材料 Fermi 能级附近的态密度，增加声子散射，实现热电性能的协同优化[143−144]，该方法在块体材料中被广泛应用，但在薄膜中的应用有待进一步探索。

与 Sb_2Te_3 基热电薄膜研究相比，Sb_2Te_3 基微型热电器件的研究还相对较少，未来需要在微型热电器件或柔性热电器件的设计开发方面展开深入研究。微型热电器件的结构一般可分为垂直结构和面内结构[17,145−146]。垂直结构的优点是吸热面积大、热能利用率高，缺点是界面电阻大、难以形成大温差。面内结构的优点是易于形成大温差、制备简单，缺点是器件吸热面积小、基底漏热和内阻较高。器件的结构对其能量转换效率等性能有着重要的影响[147]。张骐昊等[148]提出了器件优化设计逻辑框架，阐述了热电器件基本的设计原则，为器件设计提供了思路图。在器件制作成型方面也有一些问题需要解决。例如，热电材料与电极不匹配、结合状态差会降低器件的能量转换效率、可靠性和使用寿命，因此需要选择合适的电极和连接方式[149−151]；在高温端热电材料和电极的界面处容易发生相互扩散，需要在热电材料和电极之间引入过渡层[152−153]。

此外，热电薄膜的测试还存在诸多问题，薄膜材料和器件的热电性能参数测试原理及技术亟需发展完善。目前，薄膜电导率测试通常采用四探针法和范德堡法[154−156]。Seebeck 系数测试通常有微分法和积分法[157−158]。热导率的表征技术可分为 2 大类，即稳态方法和瞬态方法。其中，瞬态法又可分为时域法和频域法[138]。每种方法都有自身的优点和不足，需要综合考虑样品的尺寸、测试的温度范围、所需的测试精度等因素选择合适的方法。同时也应当注意 Sb_2Te_3 薄膜面内面外的电学和热学性能存在差异，要选择合适的方法进行测试。为了确保结果的准确性和可信度，还可以采用多种测试技术对样品进行重复测试[138]。目前还没有一种成熟的技术可以在一个样品上完成 3 个热电参数的测量，相关研究有待深入展开[150]。

当前，虽然在提升 Sb_2Te_3 基热电薄膜 ZT 值、优化热电器件结构、提升器件能量转换效率和准确测量薄膜热电性能参数等方面还存在很多困难和挑战，但是越来越多的研究人员正投身于相关研究，学科交叉越发紧密，相信未来在 Sb_2Te_3 基热电薄膜研究和应用方面会有更大的突破。

参考文献:

[1] ZHU T J, LIU Y T, FU C G, et al. Compromise and synergy in high-efficiency thermoelectric materials [J]. Adv Mater, 2017, 29(14): 1605884.

[2] LI C, JIANG F, LIU C, et al. Present and future thermoelectric materials toward wearable energy harvesting [J]. Appl Mater Today, 2019, 15: 543–557.

[3] SOLEIMANI Z, ZORAS S, CERANIC B, et al. A review on recent developments of thermoelectric materials for room-temperature applications [J]. Sustain Energy Techn, 2020, 37: 100604.

[4] YU Y, ZHU W, KONG X, et al. Recent development and application of thin-film thermoelectric cooler [J]. Front Chem Sci Eng, 2020, 14(4): 492–503.

[5] YANG L, CHEN Z G, DARGUSCH M S, et al. High performance thermoelectric materials: Progress and their applications [J]. Adv Energy Mater, 2018, 8(6): 1701797.

[6] ELSHEIKH M H, SHNAWAH D A, SABRI M F M, et al. A review on thermoelectric renewable energy: Principle parameters that affect their performance [J]. Renew Sust Energ Rev, 2014, 30: 337–355.

[7] SNYDER G J, TOBERER E S. Complex thermoelectric materials [J]. Nat Mater, 2008, 7(2): 105–114.

[8] HE J, TRITT T M. Advances in thermoelectric materials research: Looking back and moving forward[J]. Science, 2017, 357(6358): eaak9997.

[9] 张宗委, 王心宇, 刘一杰, 等. 热电能源材料研究进展[J]. 硅酸盐学报, 2018, 46(2): 288–305.
ZHANG Zongwei, WENG Xinyu, LIU Yijie, et al. J Chin Ceram Soc, 2018, 46(2): 288–305.

[10] MAO J, LIU Z, REN Z. Size effect in thermoelectric materials [J]. npj Quantum Mater, 2016, 1(1): 16028.

[11] HICKS L, DRESSELHAUS M. Use of quantum-well superlattices to obtain a high figure of merit from nonconventional thermoelectric materials [J]. MRS Online Proceedings Library, 1993, 326: 413–418.

[12] HICKS L, DRESSELHAUS M S. Thermoelectric figure of merit of a one-dimensional conductor[J]. Phys Rev B, 1993, 47(24): 16631–16643.

[13] HICKS L, DRESSELHAUS M S. Effect of quantum-well structures on the thermoelectric figure of merit[J]. Phys Rev B, 1993, 47(19): 12727–12731.

[14] FENG J J, ZHU W, DENG Y. An overview of thermoelectric films: Fabrication techniques, classification, and regulation methods [J]. Chin Phys B, 2018, 27(4): 047210.

[15] NOZARIASBMARZ A, COLLINS H, DSOUZA K, et al. Review of wearable thermoelectric energy harvesting: From body temperature to electronic systems [J]. Appl Energ, 2020, 258: 114069.

[16] DU Y, XU J Y, PAUL B, et al. Flexible thermoelectric materials and devices [J]. Appl Mater Today, 2018, 12: 366–388.

[17] YAN J, LIAO X, YAN D, et al. Review of micro thermoelectric generator [J]. J Microelectromech S, 2018, 27(1): 1–18.

[18] NOZARIASBMARZ A, SUAREZ F, DYCUS J H, et al. Thermoelectric generators for wearable body heat harvesting: Material and device concurrent optimization [J]. Nano Energy, 2020, 67: 104265.

[19] ROWE D M. CRC Handbook of Thermoelectrics [M]. Florida: CRC press, 2018: 211–213.

[20] NOLAS G S, SHARP J, GOLDSMID J. Thermoelectrics: basic principles and new materials developments [M]. New York: Springer-Verlag Berlin Heidelberg, 2013: 123–131.

[21] POUDEL B, HAO Q, MA Y, et al. High-thermoelectric performance of nanostructured bismuth antimony telluride bulk alloys [J]. Science, 2008, 320(5876): 634–638.

[22] CHEN Y, HOU X, MA C, et al. Review of development status of Bi_2Te_3-based semiconductor thermoelectric power generation [J]. Adv Mater Sci Eng, 2018, 2018: 1210562.

[23] SOLEIMANI Z, ZORAS S, CERANIC B, et al. A review on recent developments of thermoelectric materials for room-temperature applications [J]. Sustain Energy Techn, 2020, 37: 100604.

[24] KIM S I, HWANG S, ROH J W, et al. Experimental evidence of enhancement of thermoelectric properties in tellurium nanoparticle-embedded bismuth antimony telluride [J]. J Mater Res, 2012, 27(19): 2449–2456.

[25] TAN M, HAO L, LI H, et al. Approaching high-performance of ordered structure Sb_2Te_3 film *via* unique angular intraplanar grain boundaries [J]. Sci Rep, 2020, 10(1): 5978.

[26] VENKATASUBRAMANIAN R. Lattice thermal conductivity reduction and phonon localizationlike behavior in superlattice structures [J]. Phys Rev B, 2000, 61(4): 3091–3097.

[27] ZHU T J, HU L P, ZHAO X B, et al. New insights into intrinsic point defects in V_2VI_3 thermoelectric materials [J]. Adv Sci, 2016, 3(7): 1600004.

[28] TAKASHIRI M. Thin films of bismuth-telluride-based alloys [C] //Mele Paolo, Narducci Dario, Ohta Michihiro, eds. Thermoelectric Thin Films: Materials and Devices[M]. Cham: Springer International Publishing, 2019: 1–29.

[29] WITTING I T, CHASAPIS T C, RICCI F, et al. The thermoelectric properties of bismuth telluride [J]. Adv Electron Mater, 2019, 5(6): 1800904.

[30] FANG T, LI X, HU C L, et al. Complex band structures and lattice dynamics of Bi_2Te_3-based compounds and solid solutions [J]. Adv Funct Mater, 2019, 29(28): 1900677.

[31] LOŠŤÁK P, STARÝ Z, HORÁK J, et al. Substitutional defects in Sb_2Te_3 crystals [J]. Phys Status Solidi A, 1989, 115(1): 87–96.

[32] HORÁK J, DRAŠAR Č, NOVOTNÝ R, et al. Non-stoichiometry of the crystal lattice of antimony telluride [J]. Phys Stat Sol (A), 1995, 149(2): 549–556.

[33] STARÝ Z, HORÁK J, STORDEUR M, et al. Antisite defects in $Sb_{2-x}Bi_xTe_3$ mixed crystals [J]. J Phys Chem Solids, 1988, 49(1): 29–34.

[34] RIEGER F, KAISER K, BENDT G, et al. Low intrinsic *c*-axis thermal conductivity in PVD grown epitaxial Sb_2Te_3 films [J]. J Appl Phys, 2018, 123(17): 175108.

[35] GOLDSMID H J. The thermal conductivity of bismuth telluride [J]. Proc Phys Soc B, 1956, 69(2): 203–209.

[36] DELVES R T, BOWLEY A E, HAZELDEN D W, et al. Anisotropy of the electrical conductivity in bismuth telluride [J]. Proc Phys Soc, 1961, 78(5): 838–844.

[37] LEE W Y, PARK N W, AHN J Y, et al. Anisotropic behavior of the temperature-dependent thermal conductivity in p-Type bismuth antimony telluride (p-$Bi_{0.5}Sb_{1.5}Te_3$) thin films [J]. J Nanoelectron Optoelectron, 2017, 12(10): 1123–1128.

[38] MANZANO C V, ABAD B, ROJO M M, et al. Anisotropic effects on the thermoelectric properties of highly oriented electrodeposited Bi_2Te_3 films [J]. Sci Rep, 2016, 6(1): 19129.

[39] TAKAYAMA K, TAKASHIRI M. Multi-layered-stack thermoelectric

generators using p-type Sb_2Te_3 and n-type Bi_2Te_3 thin films by radio-frequency magnetron sputtering [J]. Vacuum, 2017, 144: 164−171.

[40] ZHOU A, FU Q, ZHANG W, et al. Enhancing the thermoelectric properties of the electroplated Bi_2Te_3 films by tuning the pulse off-to-on ratio [J]. Electrochim Acta, 2015, 178: 217−224.

[41] HATSUTA N, TAKEMORI D, TAKASHIRI M. Effect of thermal annealing on the structural and thermoelectric properties of electrodeposited antimony telluride thin films [J]. J Alloys Compd, 2016, 685: 147−152.

[42] ROSTEK R, STEIN N, BOULANGER C. A review of electroplating for V-VI thermoelectric films: From synthesis to device integration [J]. J Mater Res, 2015, 30(17): 2518−2543.

[43] LAL S, GAUTAM D, RAZEEB K M. Optimization of annealing conditions to enhance thermoelectric performance of electrodeposited p-type BiSbTe thin films [J]. APL Mater, 2019, 7(3): 031102.

[44] YAMASAKI I, YAMANAKA R, MIKAMI M, et al. Thermoelectric properties of Bi_2Te_3/Sb_2Te_3 superlattice structure[C] //Seventeenth International Conference on Thermoelectrics, Nagoya, Japan, 1998: 210−213.

[45] MAKALA R S, JAGANNADHAM K, SALES B C. Pulsed laser deposition of Bi_2Te_3-based thermoelectric thin films [J]. J Appl Phys, 2003, 94(6): 3907−3918.

[46] SYMEOU E, NICOLAOU C, KYRATSI T, et al. Enhanced thermoelectric properties in vacuum-annealed $Bi_{0.5}Sb_{1.5}Te_3$ thin films fabricated using pulsed laser deposition [J]. J Appl Phys, 2019, 125(21): 215308.

[47] SCHOU J. Physical aspects of the pulsed laser deposition technique: The stoichiometric transfer of material from target to film [J]. Appl Surf Sci, 2009, 255(10): 5191−5198.

[48] SHEN H, LEE S, KANG J G, et al. Thickness dependence of the electrical and thermoelectric properties of co-evaporated Sb_2Te_3 films[J]. Appl Surf Sci, 2018, 429: 115−120.

[49] TAN M, DENG Y, WANG Y. Unique hierarchical structure and high thermoelectric properties of antimony telluride pillar arrays [J]. J Nanopart Res, 2012, 14(10): 1204.

[50] TAKASHIRI M, TANAKA S, MIYAZAKI K. Improved thermoelectric performance of highly-oriented nanocrystalline bismuth antimony telluride thin films [J]. Thin Solid Films, 2010, 519(2): 619−624.

[51] TAN M, DENG Y, HAO Y. Multilayered structure and enhanced thermoelectric properties of $Bi_{1.5}Sb_{0.5}Te_3$ film with preferential growth [J]. Phys Status Solidi A, 2013, 210(12): 2611−2616.

[52] MU X, ZHOU H, HE D, et al. Enhanced electrical properties of stoichiometric $Bi_{0.5}Sb_{1.5}Te_3$ film with high-crystallinity *via* layer-by-layer *in-situ* Growth [J]. Nano Energy, 2017, 33: 55−64.

[53] ZHU W, DENG Y, WANG Y, et al. Preferential growth transformation of $Bi_{0.5}Sb_{1.5}Te_3$ films induced by facile post-annealing process: Enhanced thermoelectric performance with layered structure [J]. Thin Solid Films, 2014, 556: 270−276.

[54] TAN M, DENG Y, HAO Y. Enhanced thermoelectric properties and layered structure of Sb_2Te_3 films induced by special (0 0 *l*) crystal plane [J]. Chem Phys Lett, 2013, 584: 159−164.

[55] CAO L, WANG Y, DENG Y, et al. Facile synthesis of preferential $Bi_{0.5}Sb_{1.5}Te_{3.0}$ nanolayered thin films with high power factor by the controllable layer thickness [J]. J Nanopart Res, 2013, 15(11): 2088.

[56] ZHENG Z H, FAN P, LUO J T, et al. Enhanced thermoelectric properties of antimony telluride thin films with preferred orientation prepared by sputtering a fan-shaped binary composite target [J]. J Electron Mater, 2013, 42(12): 3421−3425.

[57] KIM M-Y, OH T-S. Preparation and characterization of Bi_2Te_3/Sb_2Te_3 thermoelectric thin-film devices for power generation [J]. J Electron Mater, 2014, 43(6): 1933−1939.

[58] TRUNG N H, SAKAMOTO K, TOAN N V, et al. Synthesis and evaluation of thick films of electrochemically deposited Bi_2Te_3 and Sb_2Te_3 thermoelectric materials [J]. Materials, 2017, 10(2): 154.

[59] SCHUMACHER C, REINSBERG K G, ROSTEK R, et al. Optimizations of pulsed plated p and n-type bi_2Te_3-Based ternary compounds by annealing in different ambient atmospheres [J]. Adv Energy Mater, 2013, 3(1): 95−104.

[60] THIET D V, QUANG N V, HAI N T M, et al. Optimizing the carrier density and thermoelectric properties of Sb_2Te_3 films by using the growth temperature [J]. J Korean Phys Soc, 2018, 72(8): 915−919.

[61] AABDIN Z, PERANIO N, WINKLER M, et al. Sb_2Te_3 and Bi_2Te_3 thin films grown by room-temperature MBE [J]. J Electron Mater, 2012, 41(6): 1493−1497.

[62] SYMEOU E, PERVOLARAKI M, MIHAILESCU C N, et al. Thermoelectric properties of $Bi_{0.5}Sb_{1.5}Te_3$ thin films grown by pulsed laser deposition [J]. Appl Surf Sci, 2015, 336: 138−142.

[63] CHANG H C, CHEN C H, KUO Y K. Great enhancements in the thermoelectric power factor of BiSbTe nanostructured films with well-ordered interfaces [J]. Nanoscale, 2013, 5(15): 7017−7025.

[64] LEE C W, KIM G H, CHOI J W, et al. Improvement of thermoelectric properties of Bi_2Te_3 and Sb_2Te_3 films grown on graphene substrate [J]. Phys Status Solidi RRL, 2017, 11(6): 1700029.

[65] ALAM H, RAMAKRISHNA S. A review on the enhancement of figure of merit from bulk to nano-thermoelectric materials [J]. Nano Energy, 2013, 2(2): 190−212.

[66] SHUAI J, MAO J, SONG S, et al. Tuning the carrier scattering mechanism to effectively improve the thermoelectric properties [J]. Energy Environ Sci, 2017, 10(3): 799−807.

[67] HU C. Modern Semiconductor Devices for Integrated circuits [M]. Upper Saddle River, NJ: Prentice Hall, 2010: 40−43.

[68] FAN P, ZHENG Z H, LIANG G X, et al. Thermoelectric characterization of ion beam sputtered Sb_2Te_3 thin films [J]. J Alloys Compd, 2010, 505(1): 278−280.

[69] KIM J, LIM J H, MYUNG N V. Composition- and crystallinity-dependent thermoelectric properties of ternary $Bi_xSb_{2-x}Te_y$ films [J]. Appl Surf Sci, 2018, 429: 158−163.

[70] FANG B, ZENG Z G, YAN X X, et al. Effects of annealing on thermoelectric properties of Sb_2Te_3 thin films prepared by radio frequency magnetron sputtering [J]. J Mater Sci-Mater El, 2013, 24(4): 1105−1111.

[71] JUNLABHUT P, NUTHONGKUM P, SAKULKALAVEK A, et al. Enhancing the thermoelectric properties of sputtered Sb_2Te_3 thick films *via* post-annealing treatment [J]. Surf Coat Technol, 2020, 387: 125510.

[72] TYNELL T, GEISHENDORF K, PIONTEK S, et al. Rapid thermal annealing of Sb_2Te_3 thin films grown *via* atomic layer deposition [J]. Thin Solid Films, 2020, 700: 137922.

[73] LIN J M, CHEN Y C, YANG C F, et al. Effect of substrate temperature on the thermoelectric properties of the Sb_2Te_3 thin films deposition by using thermal evaporation method [J]. J Nanomater, 2015, 2015: 135130.

[74] MORIKAWA S, INAMOTO T, TAKASHIRI M. Thermoelectric

properties of nanocrystalline Sb_2Te_3 thin films: Experimental evaluation and first-principles calculation, addressing effect of crystal grain size [J]. Nanotechnology, 2018, 29(7): 075701.

[75] 李秦, 檀柏梅, 张建新, 等. 退火时间对 Bi/Te 多层薄膜结构和热电性能的影响[J]. 硅酸盐学报, 2016, 44(1): 95–103.
LI Qin, TAN Baimei, ZHANG Jianxin, et al. J Chin Ceram Soc, 2016, 44(1): 95–103.

[76] KIM D-H, LEE G-H, KIM O-J. The influence of post-deposition annealing on thermoelectric properties of Bi–Sb–Te films prepared by sputtering [J]. Semicond Sci Technol, 2007, 22(2): 132–136.

[77] CHEN T B, FAN P, ZHENG Z H, et al. Influence of substrate temperature on structural and thermoelectric properties of antimony telluride thin films fabricated by RF and DC cosputtering [J]. J Electron Mater, 2012, 41(4): 679–683.

[78] GONCALVES L M, ALPUIM P, ROLO A G, et al. Thermal co-evaporation of Sb_2Te_3 thin-films optimized for thermoelectric applications [J]. Thin Solid Films, 2011, 519(13): 4152–4157.

[79] ZOU H, ROWE D M, WILLIAMS S G K. Peltier effect in a co-evaporated Sb_2Te_3(P)-Bi_2Te_3(N) thin film thermocouple [J]. Thin Solid Films, 2002, 408(1): 270–274.

[80] SILVA L W D, KAVIANY M, UHER C. Thermoelectric performance of films in the bismuth-tellurium and antimony-tellurium systems [J]. J Appl Phys, 2005, 97(11): 114903.

[81] WANG G Y, ENDICOTT L, UHER C. Recent advances in the growth of Bi-Sb-Te-Se thin films [J]. Sci Rep, 2011, 3(4): 539–560.

[82] KHUMTONG T, SAKULKALAVEK A, SAKDANUPHAB R. Empirical modelling and optimization of pre-heat temperature and Ar flow rate using response surface methodology for stoichiometric Sb_2Te_3 thin films prepared by RF magnetron sputtering [J]. J Alloys Compd, 2017, 715: 65–72.

[83] TAN M, DENG Y, HAO Y. Enhancement of thermoelectric properties induced by oriented nanolayer in $Bi_2Te_{2.7}Se_{0.3}$ columnar films [J]. Mater Chem Phys, 2014, 146(1/2): 153–158.

[84] KIM D H, BYON E, LEE G H, et al. Effect of deposition temperature on the structural and thermoelectric properties of bismuth telluride thin films grown by co-sputtering [J]. Thin Solid Films, 2006, 510(1/2): 148–153.

[85] LENSCH-FALK J L, BANGA D, HOPKINS P E, et al. Electrodeposition and characterization of nano-crystalline antimony telluride thin films [J]. Thin Solid Films, 2012, 520(19): 6109–6117.

[86] TAN M, WANG Y, DENG Y, et al. Oriented growth of A_2Te_3 (A = Sb, Bi) films and their devices with enhanced thermoelectric performance [J]. Sensor Actuat A-Phys, 2011, 171(2): 252–259.

[87] SHEN S, ZHU W, DENG Y, et al. Enhancing thermoelectric properties of Sb_2Te_3 flexible thin film through microstructure control and crystal preferential orientation engineering [J]. Appl Surf Sci, 2017, 414: 197–204.

[88] FAN P, LI R, CHEN Y-X, et al. High thermoelectric performance achieved in $Bi_{0.4}Sb_{1.6}Te_3$ films with high (0 0 *l*) orientation *via* magnetron sputtering [J]. J Eur Ceram Soc, 2020, 40(12): 4016–4021.

[89] GAYNER C, KAR K K. Recent advances in thermoelectric materials [J]. Prog Mater Sci, 2016, 83: 330–382.

[90] LV S, QIAN Z, HU D, et al. A comprehensive review of strategies and approaches for enhancing the performance of thermoelectric module [J]. Energies, 2020, 13(12): 3142.

[91] WEI Z, LI Z, LUO P, et al. Simultaneously increased carrier concentration and mobility in p-type $Bi_{0.5}Sb_{1.5}Te_3$ throng Cd doping [J]. J Alloys Compd, 2020, 830: 154625.

[92] 冯建林, 魏长平, 许洁. 掺杂金属离子对 $Ca_3Co_4O_9$ 的热电性能的影响[J]. 硅酸盐学报, 2008, 36(11): 1501–1504.
FENG Jianlin, WEI Changping, XU Jie. J Chin Ceram Soc, 2008, 36(11): 1501–1504.

[93] TAN C, TAN X, YU B, et al. Synergistically optimized thermoelectric performance in $Bi_{0.48}Sb_{1.52}Te_3$ by hot deformation and Cu doping [J]. ACS Appl Energ Mater, 2019, 2(9): 6714–6719.

[94] HAO F, QIU P F, SONG Q F, et al. Roles of Cu in the enhanced thermoelectric properties in $Bi_{0.5}Sb_{1.5}Te_3$ [J]. Materials, 2017, 10(3): 251.

[95] WEI Z, WANG C, YOU L, et al. Significantly enhanced thermoelectric performance of Cu-doped p-type $Bi_{0.5}Sb_{1.5}Te_3$ by a hydrothermal synthesis method [J]. RSC Adv, 2017, 7(65): 41111–41116.

[96] SHI D T, WANG R P, WANG G X, et al. Enhanced thermoelectric properties in Cu-doped Sb_2Te_3 films [J]. Vacuum, 2017, 145: 347–350.

[97] TAN M, DENG Y, WANG Y, et al. Fabrication of Highly (0 0 *l*)-textured Sb_2Te_3 film and corresponding thermoelectric device with enhanced performance [J]. J Electron Mater, 2012, 41(11): 3031–3038.

[98] YANG J, YIP H-L, JEN K-Y. Rational design of advanced thermoelectric materials [J]. Adv Energy Mater, 2013, 3(5): 549–565.

[99] AHMED A, HAN S. Optimizing the structural, electrical and thermoelectric properties of antimony telluride thin films deposited on aluminum nitride-coated stainless steel foil [J]. Sci Rep, 2020, 10(1): 6978.

[100] GAYNER C, AMOUYAL Y. Energy filtering of charge carriers: Current trends, challenges, and prospects for thermoelectric materials [J]. Adv Funct Mater, 2020, 30(18): 1901789.

[101] MINNICH A J, DRESSELHAUS M S, REN Z F, et al. Bulk nanostructured thermoelectric materials: Current research and future prospects [J]. Energy Environ Sci, 2009, 2(5): 466–479.

[102] ZHANG Z Q, WU Y G, ZHANG H M, et al. Enhancement of Seebeck coefficient in Sb-rich Sb_2Te_3 thin film [J]. J Mater Sci-mater El, 2015, 26(3): 1619–1624.

[103] ZHANG Y, SNEDAKER M L, BIRKEL C S, et al. Silver-based intermetallic heterostructures in Sb_2Te_3 thick films with enhanced thermoelectric power factors [J]. Nano Lett, 2012, 12(2): 1075–1080.

[104] KO D K, KANG Y J, MURRAY C B. Enhanced thermopower *via* carrier energy filtering in solution-processable Pt-Sb_2Te_3 nanocomposites [J]. Nano Lett, 2011, 11(7): 2841–2844.

[105] KIM J, LEE K H, KIM S D, et al. Simple and effective fabrication of Sb_2Te_3 films embedded with Ag_2Te nanoprecipitates for enhanced thermoelectric performance [J]. J Mater Chem A, 2018, 6(2): 349–356.

[106] ZHANG Z Q, ZHANG H M, WU Y G, et al. Optimization of the thermopower of antimony telluride thin film by introducing tellurium nanoparticles [J]. Appl Phys A-Mater, 2015, 118(3): 1043–1051.

[107] YOO I J, SONG Y, LIM D C, et al. Thermoelectric characteristics of Sb_2Te_3 thin films formed via surfactant-assisted electrodeposition [J]. J Mater Chem A, 2013, 1(17): 5430–5435.

[108] 陈立东, 刘睿恒, 史迅. 热电材料与器件[M]. 北京: 科学出版社, 2018: 34–39.

[109] KIM M-Y, OH T-S. Crystallization behavior and thermoelectric characteristics of the electrodeposited Sb_2Te_3 thin films [J]. Thin Solid Films, 2010, 518(22): 6550–6553.

[110] KIM J, ZHANG M, BOSZE W, et al. Maximizing thermoelectric properties by nanoinclusion of γ-SbTe in Sb_2Te_3 film *via* solid-state

phase transition from amorphous Sb-Te electrodeposits [J]. Nano Energy, 2015, 13: 727−734.

[111] KIM J, JUNG H, LIM J H, et al. Facile control of interfacial energy-barrier scattering in antimony telluride electrodeposits [J]. J Electron Mater, 2017, 46(4): 2347−2355.

[112] LIM S K, KIM M Y, OH T S. Thermoelectric properties of the bismuth-antimony-telluride and the antimony-telluride films processed by electrodeposition for micro-device applications [J]. Thin Solid Films, 2009, 517(14): 4199−4203.

[113] BOTTNER H, CHEN G, VENKATASUBRAMANIAN R. Aspects of thin-film superlattice thermoelectric materials, devices, and applications [J]. MRS Bull, 2006, 31(3): 211−217.

[114] WINKLER M, LIU X, SCHURMANN U, et al. Current status in fabrication, structural and transport property characterization, and theoretical understanding of Bi_2Te_3/Sb_2Te_3 superlattice systems [J]. Z Anorg Allg Chem, 2012, 638(15): 2441−2454.

[115] VENKATASUBRAMANIAN R, COLPITTS T, WATKO E, et al. Experimental evidence of high power factors and low thermal conductivity in Bi_2Te_3/Sb_2Te_3 superlattice thin-films[C] //Fifteenth International Conference on Thermoelectrics, Pasadena, USA, 1996: 454−458.

[116] VENKATASUBRAMANIAN R, SIIVOLA E, COLPITTS T, et al. Thin-film thermoelectric devices with high room-temperature figures of merit [J]. Nature, 2001, 413(6856): 597−602.

[117] HANSEN A L, DANKWORT T, WINKLER M, et al. Synthesis and thermal instability of high-quality Bi_2Te_3/Sb_2Te_3 Super lattice thin film thermoelectrics [J]. Chem Mater, 2014, 26(22): 6518−6522.

[118] KONIG J D, WINKLER M, BULLER S, et al. Bi_2Te_3-Sb_2Te_3 superlattices grown by nanoalloying [J]. J Electron Mater, 2011, 40(5): 1266−1270.

[119] BANGA D, LENSCH-FALK J L, MEDLIN D L, et al. Periodic modulation of Sb stoichiometry in $Bi_2Te_3/Bi_{2-x}Sb_xTe_3$ multilayers using pulsed electrodeposition [J]. Cryst Growth Des, 2012, 12(3): 1347−1353.

[120] PARK N W, LEE W Y, YOON Y S, et al. Achieving out-of-plane thermoelectric figure of merit ZT=1.44 in a p-type $Bi_2Te_3/Bi_{0.5}Sb_{1.5}Te_3$ superlattice film with low interfacial resistance [J]. ACS Appl Mater Interfaces, 2019, 11(41): 38247−38254.

[121] VENKATASUBRAMANIAN R, COLPITTS T, WATKO E, et al. MOCVD of Bi_2Te_3, Sb_2Te_3 and their superlattice structures for thin-film thermoelectric applications [J]. J Cryst Growth, 1997, 170(1-4): 817−821.

[122] VENKATASUBRAMANIAN R, COLPITTS T. Enhancement in figure-of-merit with superlattice structures for thin-film thermoelectric devices [J]. MRS Proceedings, 1997, 478: 73−84.

[123] CHEN G. Phonon transport in low dimensional [C]// Tritt T Med. Recent Treads in Thermoelectric Materials Research Ⅲ. New York: Elsevier, 2001: 203−259.

[124] CHEN G. Thermal conductivity and ballistic-phonon transport in the cross-plane direction of superlattices [J]. Phys Rev B, 1998, 57(23): 14958−14973.

[125] CHEN G, NEAGU M. Thermal conductivity and heat transfer in superlattices [J]. Appl Phys Lett, 1997, 71(19): 2761−2763.

[126] SIMKIN M V, MAHAN G D. Minimum thermal conductivity of superlattices [J]. Phys Rev Lett, 2000, 84(5): 927−930.

[127] LUCKYANOVA M N, GARG J, ESFARJANI K, et al. Coherent phonon heat conduction in superlattices [J]. Science, 2012, 338(6109): 936−939.

[128] GARG J, CHEN G. Minimum thermal conductivity in superlattices: A first-principles formalism [J]. Phys Rev B, 2013, 87(14): 140302.

[129] TOUZELBAEV M N, ZHOU P, VENKATASUBRAMANIAN R, et al. Thermal characterization of Bi_2Te_3/Sb_2Te_3 superlattices [J]. J Appl Phys, 2001, 90(2): 763−767.

[130] MOYZHES B, NEMCHINSKY V. Thermoelectric figure of merit of metal–semiconductor barrier structure based on energy relaxation length [J]. Appl Phys Lett, 1998, 73(13): 1895−1897.

[131] SHAKOURI A, BOWERS J E. Heterostructure integrated thermionic coolers [J]. Appl Phys Lett, 1997, 71(9): 1234−1236.

[132] HICKS L D, DRESSELHAUS M S. Effect of quantum-well structures on the thermoelectric figure of merit [J]. Phys Rev B, 1993, 47(19): 12727−12731.

[133] JIN H, LI J, IOCOZZIA J, et al. Hybrid organic-inorganic thermoelectric materials and devices [J]. Angew Chem Int Edit, 2019, 58(43): 15206−15226.

[134] CHEN S, LI F, CHEN Y X, et al. Enhanced thermoelectric properties of Sb_2Te_3/CH_3NH_3I hybrid thin films by post-annealing [J]. Inorg Chem Front, 2020, 7(1): 198−203.

[135] WEI M, CHEN T-B, HU J-G, et al. Effect of organic nano-components on the thermoelectric properties of Sb_2Te_3 nanocrystal thin film [J]. Scripta Mater, 2020, 185: 105−110.

[136] JIANG J, CHEN L, BAI S, et al. Thermoelectric properties of p-type $(Bi_2Te_3)_x(Sb_2Te_3)_{1-x}$ crystals prepared *via* zone melting [J]. J Cryst Growth, 2005, 277(1): 258−263.

[137] RIEGER F, RODDATIS V, KAISER K, et al. Transition into a phonon glass in crystalline thermoelectric $(Sb_{1-x}Bi_x)_2Te_3$ films [J]. Phys Rev Mater, 2020, 4(2): 025402.

[138] WANG H, CHU W, CHEN G. A brief review on measuring methods of thermal conductivity of organic and hybrid thermoelectric materials [J]. Adv Electron Mater, 2019, 5(11): 1900167.

[139] ABAD B, BORCA-TASCIUC D A, MARTIN-GONZALEZ M S. Non-contact methods for thermal properties measurement [J]. Renew Sust Energ Rev, 2017, 76: 1348−1370.

[140] TAN G, ZHAO L D, KANATZIDIS M G. Rationally designing high-performance bulk thermoelectric materials [J]. Chem Rev, 2016, 116(19): 12123−12149.

[141] LI J F, LIU W S, ZHAO L D, et al. High-performance nanostructured thermoelectric materials [J]. NPG Asia Mater, 2010, 2(4): 152−158.

[142] ZHOU M, LI J F, KITA T. Nanostructured $AgPb_mSbTe_{m+2}$ system bulk materials with enhanced thermoelectric performance [J]. J Am Chem Soc, 2008, 130(13): 4527−4532.

[143] 陈立东, 熊震, 柏胜强, 等. 纳米复合热电材料研究进展[J]. 无机材料学报, 2010, 25(6): 561−568.
CHEN Lidong, Xiong Zhen, BAI Shengqiang, et al. J Inorg Mater (in Chinese), 2010, 25(6): 561−568.

[144] DRESSELHAUS M S, CHEN G, TANG M Y, et al. New directions for low-dimensional thermoelectric materials [J]. Adv Mater, 2007, 19(8): 1043−1053.

[145] STARK I. Micro Thermoelectric Generators [C] //Brand O, Fedder G K, Hierold C, eds. Micro Energy Harvesting. John Wiley & Sons, 2015: 245−269.

[146] GLATZ W, SCHWYTER E, DURRER L, et al. Bi_2Te_3-based flexible micro thermoelectric generator with optimized design [J]. J Microelectromech S, 2009, 18(3): 763−772.

[147] 陈立东, 刘睿恒, 史迅. 热电材料与器件[M]. 北京: 科学出版社,

2018: 163–189.

[148] 张骐昊, 柏胜强, 陈立东, 等. 热电发电器件与应用技术：现状、挑战与展望 [J]. 无机材料学报, 2019, 34(3): 279–293.
ZHANG Qihao, BAI Shengqiang, CHEN Lidong, et al. J Inorg Mater (in Chinese), 2019, 34(3): 279–293.

[149] LIN Y-C, YANG C-L, HUANG J-Y, et al. Low-temperature bonding of $Bi_{0.5}Sb_{1.5}Te_3$ thermoelectric material with Cu electrodes using a thin-film In interlayer [J]. Metall Mater Trans A, 2016, 47(9): 4767–4776.

[150] SHI X-L, ZOU J, CHEN Z-G. Advanced thermoelectric design: From materials and structures to devices [J]. Chem Rev, 2020, 120(15): 7399–7515.

[151] 张骐昊, 刘睿恒, 廖锦城, 等. 填充方钴矿热电器件的结构优化设计与性能[J]. 硅酸盐学报, 2021, 49(2): 1–9.
ZHANG Qihao, LIU Ruiheng, LIAO Jincheng, et al. J Chin Ceram Soc, 2021, 49(2): 1–9.

[152] BAE N-H, HAN S, LEE K E, et al. Diffusion at interfaces of micro thermoelectric devices [J]. Curr Appl Phys, 2011, 11(5): S40–S44.

[153] MING G, JIEHUA W, JINCHENG L, et al. A high-throughput strategy to screen interfacial diffusion barrier materials for thermoelectric modules [J]. J Mater Res, 2019, 34(7): 1179–1187.

[154] 陈立东, 刘睿恒, 史迅. 热电材料与器件[M]. 北京: 科学出版社, 2018: 54–58.

[155] van der PAUW L J. A method of measuring the resistivity and Hall coefficient on lamellae of arbitrary shape [J]. Philips Techn Rev, 1958, 20: 220–224.

[156] HEANEY M B. Electrical conductivity and resistivity [C]// WEBSTER J G, ed. The measurement, instrumentation and sensors handbook. Bosa Roca, United States: Springer Science & Business Media, 2000: 1332–1345.

[157] WANG C, CHEN F, SUN K, et al. Contributed Review: Instruments for measuring Seebeck coefficient of thin film thermoelectric materials: A mini-review [J]. Rev Sci Instrum, 2018, 89(10): 101501.

[158] ZHOU Y, YANG D, LI L, et al. Fast Seebeck coefficient measurement based on dynamic method [J]. Rev Sci Instrum, 2014, 85(5): 054904.